peaks to zero. From Table 5, this value of n is seen to be $2/\chi_1^2$ for non-centrosymmetric and $2/(1 + \chi_1^2)$ for centrosymmetric structures. The use of this obviously depends upon knowing or obtaining an estimate of the quantity χ_1^2, the proportion of correct to total scattering power included in the structure factor calculation. It can be seen from (19) that different values of n alter the density at the P and W peaks but do not change the density at the Q peaks in relation to the background.

The β synthesis is sensitive to small values of $|F_I|$ since these give rise to very large coefficients. Ramachandran & Ayyar (1963) (see also Ramachandran & Srinivasan, 1970) have proposed an empirical weighting scheme to deal with this. However, the weighting scheme does not increase the useful information in the synthesis beyond what is shown in this paper. The weighted $2F_o - F_c$ and weighted γ' syntheses are therefore a little easier to use than the β synthesis.

The theory presented here is a little optimistic in that atoms wrongly included in the $2F_o - F_c$ and γ' syntheses are not suppressed by as much as is predicted However, the comparison with the β synthesis is valid since the same approximations in the theory apply to all the cases considered.

References

CHACKO, K. K. & MAZUMDAR, S. K. (1969). *Z. Kristallogr.* **128**, 315–320.

DEISENHOFER, J. & STEIGEMANN, W. (1975). *Acta Cryst.* B**31**, 238–250.

JACK, A., LADNER, J. E. & KLUG, A. (1976). *J. Mol. Biol.* **108**, 619–649.

KALYANARAMAN, A. R., PARTHASARATHY, S. & RAMACHANDRAN, G. N. (1969). In *Physics of the Solid State*, edited by S. BALAKRISHNA, M. KRISHNAMURTHY & B. RAMACHANDRA RAO, pp. 63–76. New York: Academic Press.

KARTHA, G., RAMACHANDRAN, G. N., BHAT, H. B., MADHAVAN NAIR, P., RAGHAVAN, V. K. V. & VENKATARAMAN, K. (1963). *Tetrahedron Lett.* 7, 459–472.

LUZZATI, V. (1953). *Acta Cryst.* **6**, 142–152.

MAIN, P. & HULL, S. E. (1978). *Acta Cryst.* A**34**, 353–361.

NIXON, P. E. & NORTH, A. C. T. (1976). *Acta Cryst.* A**32**, 320–333.

RAMACHANDRAN, G. N. & AYYAR, R. R. (1963). In *Crystallography and Crystal Perfection*, edited by G. N. RAMACHANDRAN. New York: Academic Press.

RAMACHANDRAN, G. N. & RAMAN, S. (1959). *Acta Cryst.* **12**, 957–964.

RAMACHANDRAN, G. N. & SRINIVASAN, R. (1970). *Fourier Methods in Crystallography*. London: Wiley—Interscience.

RAMAN, S. (1959). *Acta Cryst.* **12**, 964–975.

RAMAN, S. & LIPSCOMB, W. N. (1963). *Z. Kristallogr.* **119**, 30–41.

SIM, G. A. (1959). *Acta Cryst.* **12**, 813–815.

SIM, G. A. (1960). *Acta Cryst.* **13**, 511–512.

SRINIVASAN, R. (1961). *Acta Cryst.* **14**, 607–611.

WILSON, A. J. C. (1942). *Nature (London)*, **150**, 151–152.

WOOLFSON, M. M. (1956). *Acta Cryst.* **9**, 804–810.

Acta Cryst. (1979). A**35**, 785–788

X-ray Scattering Intensities from a Shell Model for Silicon

BY BRIAN F. ROBERTSON AND JOHN S. REID

Department of Natural Philosophy, The University, Aberdeen, AB9 2UE, Scotland

(*Received* 26 *March* 1979; *accepted* 1 *May* 1979)

Abstract

Accurate theoretical intensities are presented for the phonon scattering at 295 K for Si. The one-phonon and n-phonon cross sections are shown for the principal symmetry directions and the total phonon scattering contours for a section of the $(10\bar{1})$ plane. Previous total phonon calculations have been confined to materials of simpler structure and to a coarser mesh of wavevectors. The Si cross sections show general features which are expected to be seen in a wide variety of materials. These include the behaviour of the scattering near forbidden reflexions, the behaviour in three essentially different kinds of zones and the behaviour close to Bragg peaks. Results are also presented for the temperature dependence of the harmonic Debye–Waller factor.

Introduction

In spite of the widespread interest in X-ray scattering from Si, accurate kinematic phonon X-ray scattering intensity calculations have not been reported even though reasonable lattice dynamical models have been

0567-7394/79/050785-04$01.00

available for some fifteen years. One cause for the delay must be that the reliable calculation of multiphonon intensities for any scattering vector is somewhat lengthy and has only been reported for materials as simple as Al and the alkali halides (Reid & Smith, 1970*a*). With their technique on the complex eigenvectors of Si, results are reported here for shell model calculations of multiphonon X-ray scattering, one-phonon scattering and the temperature dependence of the harmonic Debye–Waller factor. The full accuracy of the model is maintained by summing over a very fine mesh of points, where appropriate.

The model used to provide the basic lattice dynamical information is the best fitted shell model II*c* of Dolling (1963). This model has been widely used by many authors and has to some extent become a standard. There are several more recent models but the best lattice dynamics model for Si has not really been established. Valence force potential models, *e.g.* Solbrig (1971), show promise, as do adiabatic bond charge models such as the recent four parameter model of Weber (1977). Hence, in fine detail some of our results will change with the use of one of the more recent models, especially if its fit includes the additional experimental data of Nilsson & Nelin (1972). However, the eigenfrequencies are the principal determining dynamical data and since the bulk of experimental data still comes from Dolling's work, then some confidence can be placed in the general level and trends in the scattering intensities.

The calculations

Of the three quantities mentioned, the multiphonon scattering deserves some preliminary comment. It is customary to expand the phonon scattering into a series in which the nth term represents the n-phonon scattering and then to simplify drastically the third and higher order terms. With care this method works for small scattering vectors or near Bragg peaks but with a lattice dynamical model it is an unnecessary approximation. The results given here are a direct calculation of the exact expression for the total harmonic scattering cross-section for a given scattering vector **K**. The complete expression (Reid & Smith, 1970*a*) involves a sum over the real space lattice and, for each real space point, a sum over reciprocal space. Most of the Si results were calculated with a real lattice containing 32 000 atoms and hence a sample of 192 000 phonon states in the Brillouin zone. Such a fine mesh ensures that the sampling errors are substantially $<1\%$, but, even using the symmetry of the Si lattice, the computation takes a considerable time.

It is believed that this is the first time that the total phonon scattering cross-section has been exactly evaluated for a non-symmorphic structure. In fact it was found that the complex eigenvectors of Si do not greatly complicate the calculation because the centre of symmetry in the underlying Bravais lattice ensures that the sums over reciprocal space are all real. Our experience confirms that it would be practical to use the method on a material of lower symmetry with several atoms per unit cell. The zero phonon expression, which is important for both the multiphonon scattering and the Debye–Waller factor, is marginally simpler than for the alkali halide case. However, the greater anisotropy of Si suggests that the integration over the dispersionless part of the acoustic branches could be improved by a more detailed evaluation. A minor improvement was incorporated but the problem was effectively avoided by the use of the very fine mesh of sample points in the summations, which reduced the zero phonon contribution to $<1\%$.

It is particularly important in a calculation which cannot be checked by hand that one has confidence in the correctness of the final answer. Apart from the usual tests and internal consistency checks, the following comparisons were always made. The summations for the multiphonon scattering also yielded the Debye–Waller factor, the one-phonon scattering and the Bragg scattering. Of these, the first two were always compared with independent and direct calculations of these quantities and found to agree to machine accuracy, while the Bragg scattering was checked to be zero to machine accuracy at all points between Bragg peaks. The results were checked to be identical for all symmetry-related **K** and the convergence of the results with increasing microcrystal size was also closely watched. With the relevant input data the correct results continued to be obtained for the alkali halides. This summarizes a stringent set of tests which such a calculation should pass.

Results

Table 1 lists the harmonic Debye–Waller factors given by the Dolling shell model as determined by a direct sum using frequencies at 512 000 wavevectors in the

Table 1. *Harmonic Debye–Waller factors given by Dolling's best fitted shell model*

Temperature (K)	B (Å^2)	Temperature (K)	B (Å^2)
1·0	0·1937	250·0	0·4514
5·0	0·1937	295·0	0·5192
10·0	0·1939	350·0	0·6038
20·0	0·1947	400·0	0·6819
40·0	0·1999	500·0	0·8402
60·0	0·2116	600·0	1·0001
80·0	0·2286	700·0	1·1610
100·0	0·2491	800·0	1·3226
150·0	0·3100	900·0	1·4847
200·0	0·3786	1000·0	1·6470

Brillouin zone. The zero phonon term was incorporated (Reid & Smith, 1970*b*) and was found to contribute about 0·5% at room temperature, falling off at lower temperatures. No corrections were attempted for a quasiharmonic frequency shift with temperature.

The Dolling model Debye–Waller factors are disappointingly high compared with the experimental value of 0·4613 at 293·2 K (Aldred & Hart, 1973). A likely cause for much of the discrepancy seems to be a systematic error in the low frequency modes of the Dolling model. Nilsson & Nelin (1972) have already pointed out that measurements may be higher than model frequencies by approximately 15% in this region. Unfortunately, such an error in the dispersionless region implies an error of some 10% in the calculated Debye–Waller factors at high temperature, due to the dominance of the low frequency contributions in the sum. This is almost exactly the difference between our calculations and the Aldred & Hart measurements.

For the calculation of the scattering intensities, the experimentally determined Debye–Waller factors of Aldred & Hart (1973) were used. Scattering factors, with the small Hönl correction for Mo radiation, were taken from *International Tables for X-ray Crystallography* (1974). These scattering factors are spherically symmetric and hence the forbidden reflexions 222, 666, 200 *etc.* will show zero Bragg intensity, but, nevertheless a significant phonon intensity averaged over a region surrounding these special reciprocal lattice vectors.

Figs. 1, 2 and 3 show the intensities in electron units per cell of the single phonon and multiphonon scattering along the three principal symmetry directions at room temperature (295 K). The plotted points are primary calculations and not interpolations. The curves show that the multiphonon scattering rises from zero at $\mathbf{K} = 0$ fairly sharply so that by $\sin\theta/\lambda = 1{\cdot}0$ it is generally larger than the single phonon scattering, except near non-zero Bragg peaks. The multiphonon scattering also peaks sharply under the Bragg reflexions but the peaking occurs much closer to the reflexion than with the single phonon scattering, being sometimes barely visible at one tenth of the distance out to the zone boundary. The obvious exception at the forbidden reflexions is due to the cancellation of the acoustic branch scattering by the forbidden structure factor while maintaining scattering from the optic branches.

Table 2 shows the phonon scattering which would be detected from a spherical region occupying 1/4000 of the Brillouin zone centred around the lower Bragg peaks along the principal symmetry directions. The scattering is expressed as a ratio to the corresponding kinematic Bragg intensity and, as explained by Reid (1973), can be used as an estimate of the diffuse scattering seen by a counter of finite width as it is scanned through the peak.

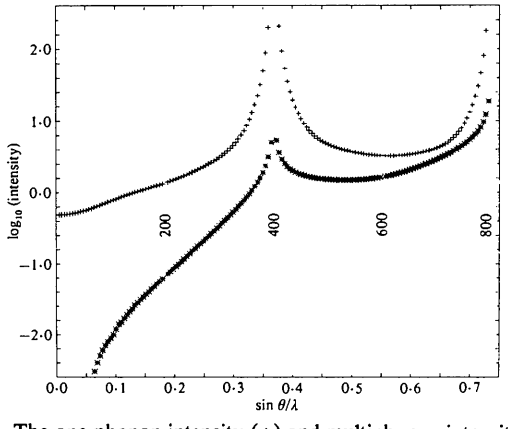

Fig. 1. The one-phonon intensity (+) and multiphonon intensity (*) on a logarithmic scale for scattering vectors along [100]. The centre of each symbol gives the intensity in electron units/cell. The points are plotted at equal intervals of h,0,0 with 20 points from Bragg peak (positions shown) to zone boundary.

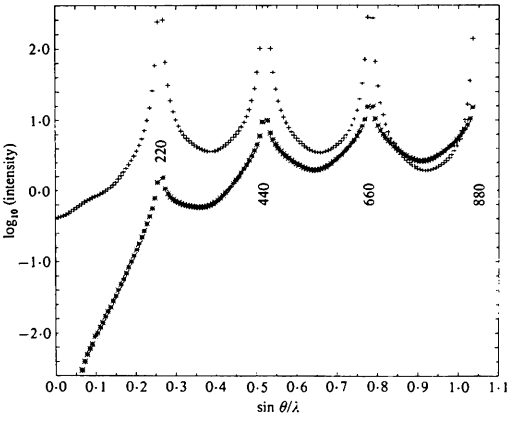

Fig. 2. As for Fig. 1 but along [110].

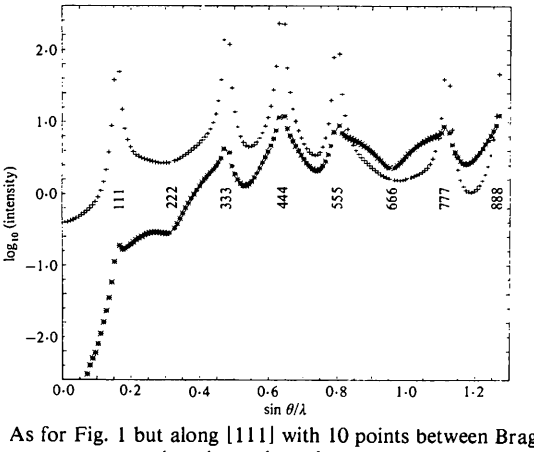

Fig. 3. As for Fig. 1 but along [111] with 10 points between Bragg peak and zone boundary.

Fig. 4 is a contour map of the total phonon scattering (one-phonon plus multiphonon) in a region of the (10$\bar{1}$) plane. The general shape and levels of the contours agree well with the experimental data of Bonefačić (1969), except of course in the region around 222. In fact the agreement is very much better than that achieved by Bonefačić's own model calculations. However, the single phonon intensities in this region, and the multiphonon intensities everywhere, require a knowledge of the off-symmetry frequencies and the complex eigenvectors appropriate to the two kinds of atomic sites. Supplying accurate values for these is a stringent test of the adequacy of the lattice dynamics model and it is a test which has not really been applied to even the most recent models, basically due to a lack of detailed experimental data. Now that the total phonon scattering can be calculated with confidence, there is an obvious call for further experimental evidence to assist in distinguishing the predictions of different models. An extensive programme of absolute intensity measurements is already under way (Robertson, Pirie & Reid, 1978) which should provide, amongst other things, some of the necessary evidence

Table 2. *The ratio* (I_{TDS}/I_{Bragg}) *expressed as a percentage*

The TDS is integrated over a sphere surrounding the Bragg reciprocal lattice vector (*hkl*), the sphere occupying 1/4000 of the Brillouin zone volume. For scaling to other volumes see Reid (1973).

h k l	I_{TDS}/I_{Bragg} %
4 0 0	0·36
8 0 0	1·45
2 2 0	0·18
4 4 0	0·72
6 6 0	1·63
8 8 0	2·94
1 1 1	0·07
3 3 3	0·61
4 4 4	1·09
5 5 5	1·71
7 7 7	3·41
8 8 8	4·46

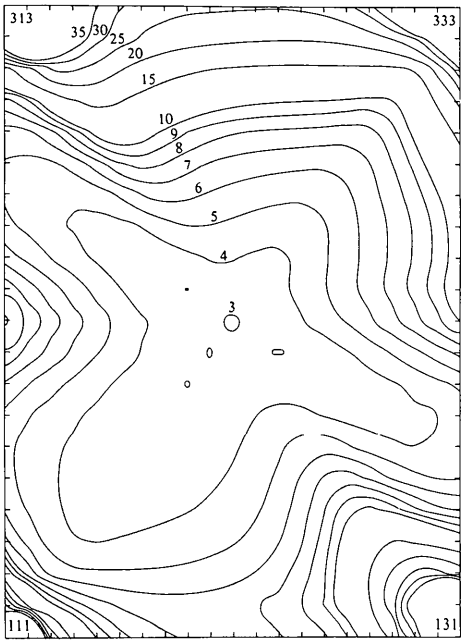

Fig. 4. Total phonon scattering in a section of the (10$\bar{1}$) plane. The contours are at electron unit/cell values of 3 to 10 in steps of 1 and 10 to 35 in steps of 5. The primary data were calculated at 441 uniformly spaced points covering the area.

Conclusion

A sample of some room temperature X-ray scattering intensities have been presented in graphical form. The authors can answer modest requests for raw numerical data over a range of temperature.

Thanks are due to Dr J. D. Pirie both for providing the lattice dynamical data and for helpful discussions. The calculations were performed on the Honeywell 66/80 of Aberdeen University as part of a project under Science Research Council grant support.

References

ALDRED, P. J. E. & HART, M. (1973). *Proc. R. Soc. London Ser. A*, **332**, 239–254.

BONEFAČIĆ, A. (1969). *Acta Cryst.* A**25**, 589–594.

DOLLING, G. (1963). *Inelastic Scattering in Solids and Liquids* **1**, 37–47. Vienna: I.A.E.A.

International Tables for X-ray Crystallography (1974). Vol. IV. Birmingham: Kynoch Press.

NILSSON, G. & NELIN, G. (1972). *Phys. Rev. B*, **6**, 3777–3786.

REID, J. S. (1973). *Acta Cryst.* A**29**, 248–251.

REID, J. S. & SMITH, T. (1970*a*). *J. Phys. C*, **3**, 1513–1526.

REID, J. S. & SMITH, T. (1970*b*). *J. Phys. Chem. Solids*, **31**, 2689–2697.

ROBERTSON, B. F., PIRIE, J. D. & REID, J. S. (1978). *Acta Cryst.* A**34**, S288.

SOLBRIG, A. W. (1971). *J. Phys. Chem. Solids*, **32**, 1761–1768.

WEBER, W. (1977). *Phys. Rev. B*, **15**, 4789–4803.